Neuropeptides 78 (2019) 101972

Contents lists available at ScienceDirect

Neuropeptides

journal homepage: www.elsevier.com/locate/npep

Ghrelin fiber projections from the hypothalamic arcuate nucleus into the dorsal vagal complex and the regulation of glycolipid metabolism

Manqing Su[a], Meixing Yan[b], Yanling Gong[a,*]

[a] Department of Pharmacy, College of Chemical Engineering, Qingdao University of Science and Technology, Qingdao 266042, China
[b] Qingdao Women and Children's Hospital, Qingdao 266042, China

ARTICLE INFO

Keywords:
Ghrelin
Glucose-sensitive neurons
Glycolipid metabolism
Dorsal vagal complex
Arcuate nucleus

ABSTRACT

Objectives: This study aimed to explore the involvement of the ghrelin pathway from the arcuate nucleus (ARC) to the dorsal vagal complex (DVC) and to determine its role in the regulation of glycolipid metabolism.
Methods: The protein and mRNA expression of ghrelin and growth hormone (GH) secretagogue receptor type 1a (GHSR-1a) were measured using immunohistochemistry and the polymerase chain reaction (PCR) method, respectively. Ghrelin fiber projections arising from the ARC and projecting into the DVC were investigated using retrograde tracing, combined with fluorescence immunohistochemical staining. The effects of electrical stimulation (ES) of the ARC on ghrelin-responsive, glucose-sensitive DVC neurons, glycolipid metabolism, and liver lipid enzymes were determined using electrical physiological method, biochemical analysis, quantitative real-time PCR (qRT-PCR) and Western blot analysis.
Results: GHSR-1a was expressed in the DVC neurons. Ghrelin fibers originating from the ARC projected into the DVC. ES of the ARC-activated the ghrelin-responsive glucose-excited (GE) and glucose-inhibited (GI) neurons in the DVC. ES of the ARC significantly elevated the serum triglyceride (TG), total cholesterol (TC), low-density lipoprotein cholesterol (LDL-C), and glucose levels; it reduced the serum high-density lipoprotein (HDL−C) and insulin levels. Moreover, ES of the ARC increased liver acetyl-CoA carboxylase-1 (ACC-1) and decreased carnitine palmitoyltransferase-1 (CPT-1) expression, resulting in lipid accumulation in the liver. All the aforementioned effects were partially blocked by pretreatment with the ghrelin receptor antagonist [D-Lys-3]-GHRP-6 in the DVC and were reduced by vagotomy. ES of the ARC increased agouti-related protein (AgRP)/neuropeptide Y (NPY) expression in the ARC and ghrelin expression in the DVC.
Conclusion: Ghrelin fiber projections arising from the ARC and projecting into the DVC play a role in the regulation of afferent glucose metabolism and glycolipid metabolism via the ghrelin receptor GHSR-1a in the DVC.

1. Introduction

Ghrelin is a 28-amino acid peptide derived from preproghrelin, a 117-amino acid precursor produced by X/A-like cells in the gastric oxyntic glands in the stomach (Colldén et al., 2017). Ghrelin is an important orexigenic peptide that regulates appetite, food intake, glucose and lipid hemostasis, and energy balance, in addition to promoting growth hormone (GH) release (Varela et al., 2011; Lv et al., 2018). Recently, the role of ghrelin in glycolipid metabolism has attracted a significant amount of research attention because pharmacological inhibition of ghrelin signaling might have therapeutic value for improving insulin resistance and treating type 2 diabetes (Poher et al., 2018).

Hypothalamic nuclei, especially the arcuate nucleus (ARC), form interconnected neuronal circuits and react to changes in energy status by regulating the expression of agouti-related protein (AgRP)/neuropeptide Y (NPY) and proopiomelanocortin, ultimately leading to changes in food intake (Paeger et al., 2017). These neurons integrate information from peripheral signals, including changes in the levels of nutrients/metabolites, such as glucose, fatty acids, and amino acids, which could be detected through nutrient-sensing mechanisms (Blouet and Schwartz, 2010). They also integrate information from various hormones, such as leptin, ghrelin, insulin, glucagon-like peptide 1, cannabinoids, glucocorticoids, and adiponectins (Diéguez et al., 2009). These processes control food intake as well as peripheral energy expenditure, body fat content, and glucose production (Morgan et al., 2004; Pocai et al., 2005; Folmes and Lopaschuk, 2007; Le Foll et al., 2009). In a previous study, ghrelin blockade in neonatal mice resulted

* Corresponding author.
E-mail address: hanyu_ma@126.com (Y. Gong).

https://doi.org/10.1016/j.npep.2019.101972
Received 20 February 2019; Received in revised form 11 September 2019; Accepted 14 September 2019
Available online 15 September 2019

in increased ARC neural projections and long-term metabolic effects, including increased body weight, visceral fat, and blood glucose levels, and decreased leptin sensitivity (Steculorum et al., 2015).

The dorsal vagal complex (DVC) is located mainly in the dorsomedial caudal medulla. The DVC is composed of the area postrema (AP), the nucleus tractus solitarius (NTS), and the dorsal motor nucleus of the vagus (DMNV). These three parts play a role in brain stem signaling that is associated with the vomiting center (Babic and Browning, 2014; Cornejo et al., 2018). The pancreas is innervated by the parasympathetic nerve fibers originating from the DVC (Delhanty and Van, 2011). These nerve fibers modulate pancreatic secretion via cholinergic and neuropeptide synapses (Delhanty and Van, 2011). The DVC contains ghrelin-sensitive neurons that mediate the effect of orexigenic agents and pancreatic enzyme secretion (Delhanty and Van, 2011). Wang et al. (2008) reported that the NTS contained ghrelin-regulated gluco-sensory neurons, and that ghrelin inhibited glucose-inhibited (GI) and glucose-excited (GE) neural innervation in the NTS. However, the mechanism in which these ghrelin-induced effects on GI and GE neurons lead to feedback regulation on insulin is unclear (Wang et al., 2008). Although ghrelin is known to play an important role in the central controlling energy homeostasis, its role in sensing glucose signaling and regulating glycolipid metabolism in mammals still needs to be fully clarified. Therefore, the present study aimed to investigate the involvement of the ghrelin pathway from the ARC to the DVC in glycolipid metabolism.

2. Materials and methods

2.1. Animals

All the animal experiments were performed according to the guidelines of Qingdao University of Science and Technology for the use of experimental animals.

Adult male wild-type (WT) Wistar rats (n = 260) were purchased from Qingdao Daren Fortune Animal Technology Co., Ltd. (Qingdao, China). The GH secretagogue receptor knock-out (GHSR-KO) rats and WT littermates were supplied by Transposagen Biopharmaceuticals, Inc. (Lexington, KY, USA) (Cahill et al., 2014), and the ghrelin-KO rats and WT littermates were supplied by the Australian Phenomics Network CRISPR service, Monash University (Pustovit et al., 2017). The animals weighed between 280 g and 330 g, and they were housed singly in cages in a temperature-controlled room (22–25 °C), with cellulose bedding and access to food and water ad libitum under a light-dark cycle (12:12 h, lights on at 8:00 a.m.), unless otherwise indicated. The rats were adaptively fed for 7 d before the experiments.

2.2. Retrograde tracing and fluorescence immunohistochemical staining

2.2.1. Fluorochrome (FG) microinjection into the DVC

The WT littermates (n = 3) were fixed on a brain stereotaxic device (Narashige SN-3, Tokyo, Japan) after being anesthetized with 20% ethyl carbamate (5 ml/kg, i.p.). A single dose of 0.2 μl of 3% (w/v) FG (Fluorochrome, Sigma, St. Louis, MO, USA) was selectively microinjected into the DVC (bregma: P: 13.68–14.28 mm, L(R): 0–0.84 mm, DV: 7.23–8.0 mm) using the atlas of Watson and Charles (Paxinos and Watson, 2008). The ghrelin-KO rats were microinjected with the same volume of saline.

2.2.2. Perfusion fixation of the brain and stomach

The brains and stomachs were harvested 7 d after the FG microinjection or the adaptive feeding. The rats were perfused through the heart with 200 ml of saline, followed by 350 ml of 4% paraformaldehyde solution formulated with a 0.1% phosphate buffer (pH 7.4). The brains and stomachs were then soaked in fixative at 4 °C for 12 h. Subsequently, the tissues were removed and placed in a 30% sucrose solution. Then, the tissues were quickly frozen in Tissue-Tek optimal cutting temperature compound (O.C.T. Compound; Sakura Finetechnical Co. Ltd., Chuo-ku, Tokyo, Japan) and cut into 15-μm-thick coronal sections on a cryostat (Microm HM 500; Microm, Heidelberg, Germany).

2.2.3. Fluorescence immunohistochemistry

The sections were incubated for 12 h. For fluorescence immunohistochemical analysis of ghrelin in the ARC, rabbit anti-ghrelin antibody (monoclonal, dilution: 1:100; Abcam, Cambridge, MA, USA) was used as the primary antibody and incubated at 4 °C for 40 h. FG-labeled goat anti-rabbit IgG secondary antibody (Cy3 conjugated, dilution: 1:500; Bioss, Beijing, China) was then added, and the sections were incubated for 2 h. To visualize the neurons, NeuN staining was performed simultaneously with ghrelin staining. Mouse anti-NeuN antibody (monoclonal, dilution: 1:300; Arigo, Taiwan, China) and rabbit anti-ghrelin receptor antibody (polyclonal, Dilution: 1:500; Bioss, Beijing, China) were used as the primary antibodies, and goat anti-mouse IgG (FITC conjugated, dilution: 1:100; Bioss, Beijing, China) and goat anti-rabbit IgG (Cy3-conjugated, dilution: 1:500; Bioss, Beijing, China) were used as the secondary antibodies. To verify the primary antibody, abundant ghrelin peptide (Abcam, Cambridge, MA, USA) and the GHSR protein (Abcam, Cambridge, MA, USA) were mixed with the anti-ghrelin antibody and the anti-GHSR antibody, and then incubated at 4 °C, overnight, respectively, before application.

The samples were observed under a CKX53 microscope (Olympus, Tokyo, Japan). Images were obtained using a DP80 digital camera (Olympus). The cells were counted using an image analysis system (Jeda Science and Technology Company, Nanjing, China). The number of labeled cells in the ARC was counted under five, high-magnification microscopic fields, and the average was calculated. The percentage of the double-labeled cells (%) = the numbers of double-labeled cells/the numbers of ghrelin-positive neurons × 100%.

2.3. Polymerase chain reaction (PCR) assay for GH secretagogue receptor type 1a (GHSR-1a)

RNA was extracted (Qiagen RNeasy Plus Mini Kit; QIAGEN, Germantown, MD, USA), reverse transcribed (Roche Transcriptor High Fidelity cDNA Synthesis Kit; Roche Applied Science, Indianapolis, IN, USA), and subjected to PCR amplification with GHSR-1a primers (5′-CTCATCGGG-AGGAAGCTATG-3′ sense and 5′-CAGGTTGCAGTA CTG-GCTGA-3′ antisense) (Xu et al., 2014). The PCR products were detected using electrophoresis on 2% agarose gel containing ethidium bromide.

2.4. Neuronal discharge recording

2.4.1. Brain surgery

The rats were fixed on a brain stereotaxic device (Narishige SN-3; Tokyo, Japan) after being anesthetized with 20% ethyl carbamate (5 ml/kg, i.p.). The skull was exposed fully, and the representative regions of the hypothalamus ARC (bregma: P: 2.12–4.30 mm, L(R): 0–0.7 mm, DV: 9.8–10.3 mm) and DVC (as described in Section 2.2.1) were drilled. The recording sites and administration of [D-Lys-3]-GHRP-6 were described in Section 2.2.1. The dura mater was removed to expose the surface of the brain, and the surface of the skull was flushed with agar physiological saline, which protected the cortex, improved the stability of the nerve recordings, and served as a localization mark of the surface of the skull.

2.4.2. Glass microelectrode preparation and drug delivery

A four-tube microelectrode (tip diameter of about 3–10 μm and electrode impedance of 5–20 mω) was used for the electrophysiological recordings and microinjection in the DVC. The recording electrode was filled with 0.2% guanamine sky blue (pH 7.7); the three other tubes were connected to a four-channel pressure injection device, and

successively filled with 15 nmol/L of ghrelin, 28 nmol/L of [D-Lys-3]-GHRP-6 (GHSR antagonist, Sigma-Aldrich Chemical Co., St. Louis, MO, USA), and 0.5 mol/l of NaCl solution. The latter was used to eliminate the effects of osmotic pressure and to exclude cells that responded to Na^+ and Cl^-.

2.4.3. Electrical stimulation (ES) of the ARC

ES was performed during the recording of the discharge of glucose-sensitive neurons in the DVC. The stimulation electrode was inserted into the ARC with reference to the atlas of Paxinos and Watson (as described in Section 2.2.1). The ES parameters were as follows: 0.5 ms in width, 20 μA in intensity, and a frequency of 50 Hz for 10 s. For the sham stimulation (SS), the electrode was buried, but no current was passed through. At the end of the experiment, the brain was removed and coronally sectioned. The ES sites were noted. Only data obtained from the rats whose electrodes were in the ARC were included in the statistical analysis.

2.4.4. Recording of the discharges from the glucose-sensing neurons

After a one-week recovery from brain surgery, the glucose-sensitive neurons in the DVC were identified by their activity in response to the 5 mM glucose solution, and 0.9% NaCl was administered as a control. To ensure that the baseline firing was stable, a period of at least 3 min was allowed to elapse before application, and 120 s of baseline data were collected before the application. Neurons were identified as GE or GI based on an increase or decrease in the firing rate of at least 20%, respectively. One-hundred-sixty-four rats were used for the glucose-sensitive neuron recording in the DVC. Only data from rats with ES sites in the ARC and injection sites in the DVC were included in the analysis.

2.5. Determination of the blood biochemical parameters

Sixty-four rats were randomly divided into eight groups ($n = 8$): ES group, SS group, ES and normal saline (ES + NS) group, SS and NS (SS + NS) group, ES and [D-Lys-3]-GHRP-6 (ES + [D-Lys-3]-GHRP-6) group, SS and [D-Lys-3]-GHRP-6 (SS + [D-Lys-3]-GHRP-6) group, SS and BIM-28163 (GHSR-1a specific antagonist, Ipsen, Australia) group (SS + BIM-28163), and ES and BIM-28163 (ES + BIM-28163) group. Either SS or ES in the ARC was performed. Moreover, 1.0 μl [D-Lys-3]-GHRP-6 (2500 nmol/l) or BIM-28163 (1250 nmol/l) was microinjected into the DVC before ES or SS. An equal volume of 0.9% saline was microinjected as a control.

After the experiment, serum samples were collected 0 h, 2 h, 4 h, and 6 h after ES in the ARC to determine the blood biochemical parameters. The serum samples were then stored at −20 °C. Subsequently, blood glucose, total cholesterol (TC), high-density lipoprotein (HDL-C), low-density lipoprotein cholesterol (LDL-C), and triglyceride (TG) levels were evaluated using a biochemical auto-analyzer (Dimension RxL Max; Siemens Healthineers, Erlangen, Germany). The serum insulin level was measured using a rat insulin enzyme-linked immunosorbent assay (ELISA) kit (Sigma-Aldrich, Merck KGaA, Darmstadt, Germany).

2.6. Vagotomy

To verify whether the effect of DVC on the glycolipid metabolism was related to afferent nerve fibers from the hypothalamus to the pancreas, vagoctomy was performed to observe the effect of ES of the ARC on the insulin levels. Thirty-two rats were divided into the following four groups ($n = 8$): SS and vagotomized (SS + vago) group, ES and vagotomized (ES + vago) group, SS and sham surgery (SS + sham) group, and ES and sham surgery (ES + sham) group.

The rats were anesthetized with 20% urethane (5 ml/kg, i.p.), and a midline abdominal incision was made to expose the subdiaphragmatic vagus nerve trunk. The stomach was gently removed and covered with moistened sterile gauze. The vagus nerve trunk was ligated with 3–0 silk sutures at the proximal and distal parts, and separated between 2 silk sutures. The peritoneal and skin incisions were closed with 6–0 silk sutures. In the rats in the SS groups, the vagus nerve trunk was exposed and separated from the surrounding tissue, but not transected. After surgery, the animals were returned to their cage until ES of the ARC was performed (Section 2.4.3) the following day.

2.7. Quantitative real-time PCR (qRT-PCR) assay for liver enzymes

Six hours after the experiment (Section 2.4.3), the livers were removed and stored at −80 °C until the liver enzyme analysis was conducted. The mRNA expression of carnitine palmitoyltransferase-1 (CPT-1) and of acetyl-CoA carboxylase-1 (ACC-1) in the liver was detected using qRT-PCR. The following published primer sequences were used: CPT-1 (F: 5′-CAGCTCGCACATTACAAGGA-3′, R: 5′-TGCACAAAGTTGC AGGACTC-3′), ACC-1 (F: 5′-TGAGGAGGACCGCATTTATC-3′, R: 5′-GCATGGAATGGCAGTAAGGT-3′). Total RNA was extracted from the liver samples, and the concentration and purity of the RNA were determined. Single-stranded cDNA was synthesized. Quantification of mRNA was done using a CFX96 real-time PCR system (Bio-Rad, Hayward, CA, USA). All procedures were performed in duplicate, and in accordance with the manufacturers' instructions.

2.8. Western blot for AgRP/NPY in the ARC and ghrelin in the DVC

Six hours after performing ES of the ARC, the DVC and ARC tissues of the rats were collected to determine the protein expression of AgRP/NPY in the ARC and ghrelin in the DVC. The collected tissue samples were accurately weighed to 100 mg, and a lysis buffer was added to extract the protein. The concentration of the protein sample was measured using a quinolinic acid test. The protein sample was electrophoresed on Tris-trimethylglycine; it was then transferred to a nitrocellulose transfer membrane and blocked with a blocking solution for 1 h. Primary antibody (rabbit polyclonal, anti-AgRP antibody, dilution: 1:800; anti-NPY antibody, dilution: 1:800; anti-ghrelin antibody, dilution: 1:250, Abcam, Cambridge, MA, USA) was added, and the samples were incubated overnight at 4 °C. The membrane was washed with Tris-Buffered Saline and Tween 20 (TBST) membrane buffer (10 min/time, five times), and then horse radish peroxidase (HRP)-labeled goat anti-rabbit IgG secondary antibody (Abcam, Cambridge, MA, USA, 1:5000) was added for 1 h at room temperature. Following the application of chemiluminescent peroxidase, the Western blots were analyzed using X-ray film. The film optical density was measured using OptiQuant software; it was normalized using parallel Western blots with glyceraldehyde 3-phosphate dehydrogenase (GAPDH) (Abcam, Cambridge, MA, USA, 1:1000).

2.9. Histochemical verification

At the end of the ES experiment, a direct current (50 μA, 20 min) was passed through the electrode. Iron deposits of pontamine sky blue were used to check the electrode recording sites. To verify the microinjection sites or the recording sites in the DVC, 0.5 μl of pontamine sky blue was microinjected either directly or through a cannula at the end of the experiment. After perfusion and fixation of the brain, 50 μm of the frozen coronal sections were cut through various regions of the ARC (Fig. 1A, B) or DVC (Fig. 1C, D), and then observed under a light microscope. Two incorrect ES positions were located in the ventromedial hypothalamic nucleus (VMH) (Fig. 1E, F, G, H).

2.10. Statistical analysis

Data are expressed as the mean ± standard error of the mean. Statistical comparisons were performed using an independent sample *t*-test and a one-way analysis of variance, followed by post-hoc multiple comparison tests. GraphPad Prism version 5 software (GraphPad Software, Inc., La Jolla, CA, USA) was used to make the statistical

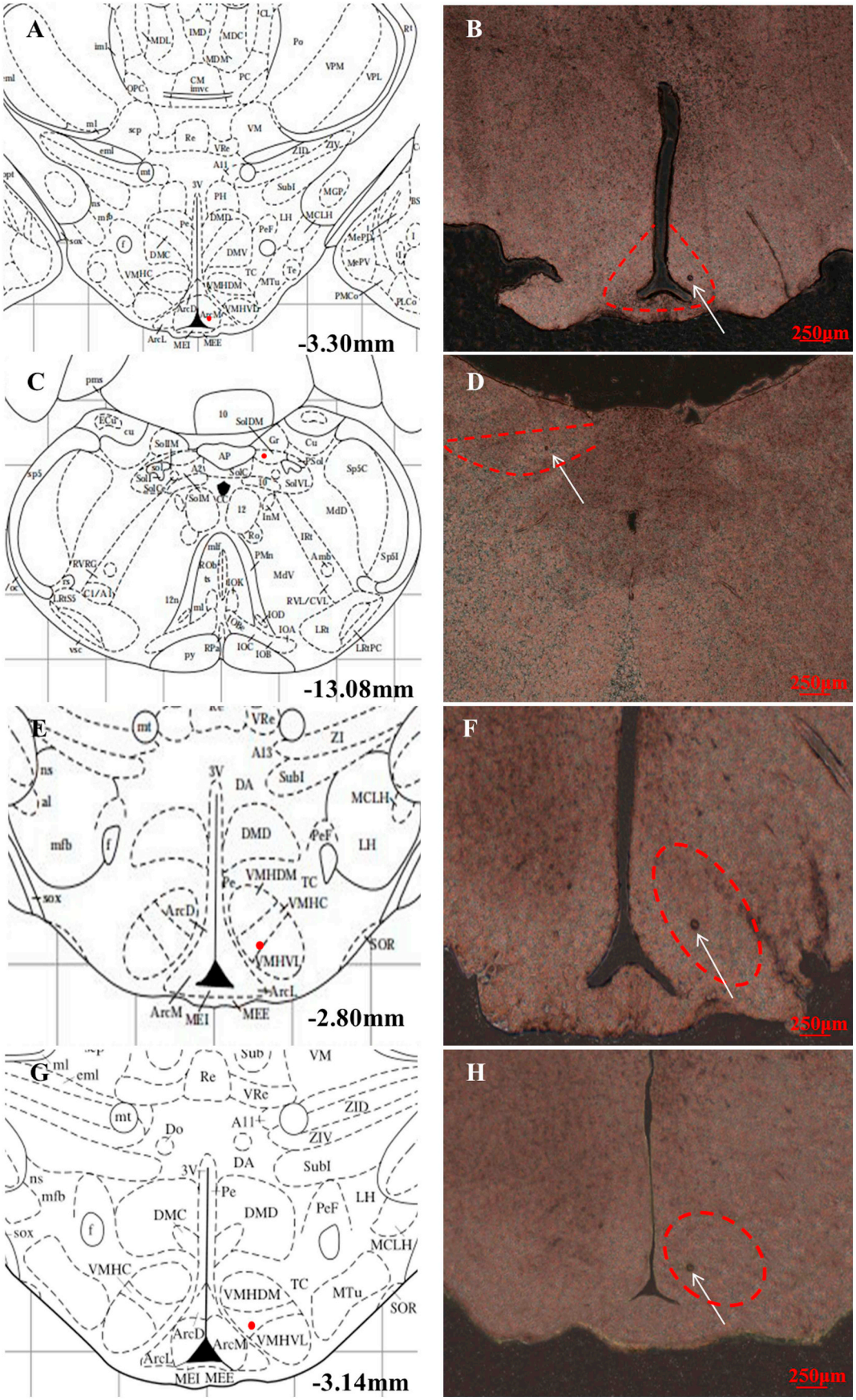

Fig. 1. Histological verification of the electrical stimulation (ES) sites and microinjection or recording sites.
The correct locations of the ES sites in the ARC (A), the microinjection or recording sites in the DVC (C) and two incorrect locations of ES sites in the VMH (E and G) are shown as dots on the brain atlas. A typical photomicrograph showing pontamine sky blue deposits in the correct ES sites (B), microinjection or recording sites (D) and incorrect ES sites. Scale bars, 250 μm.

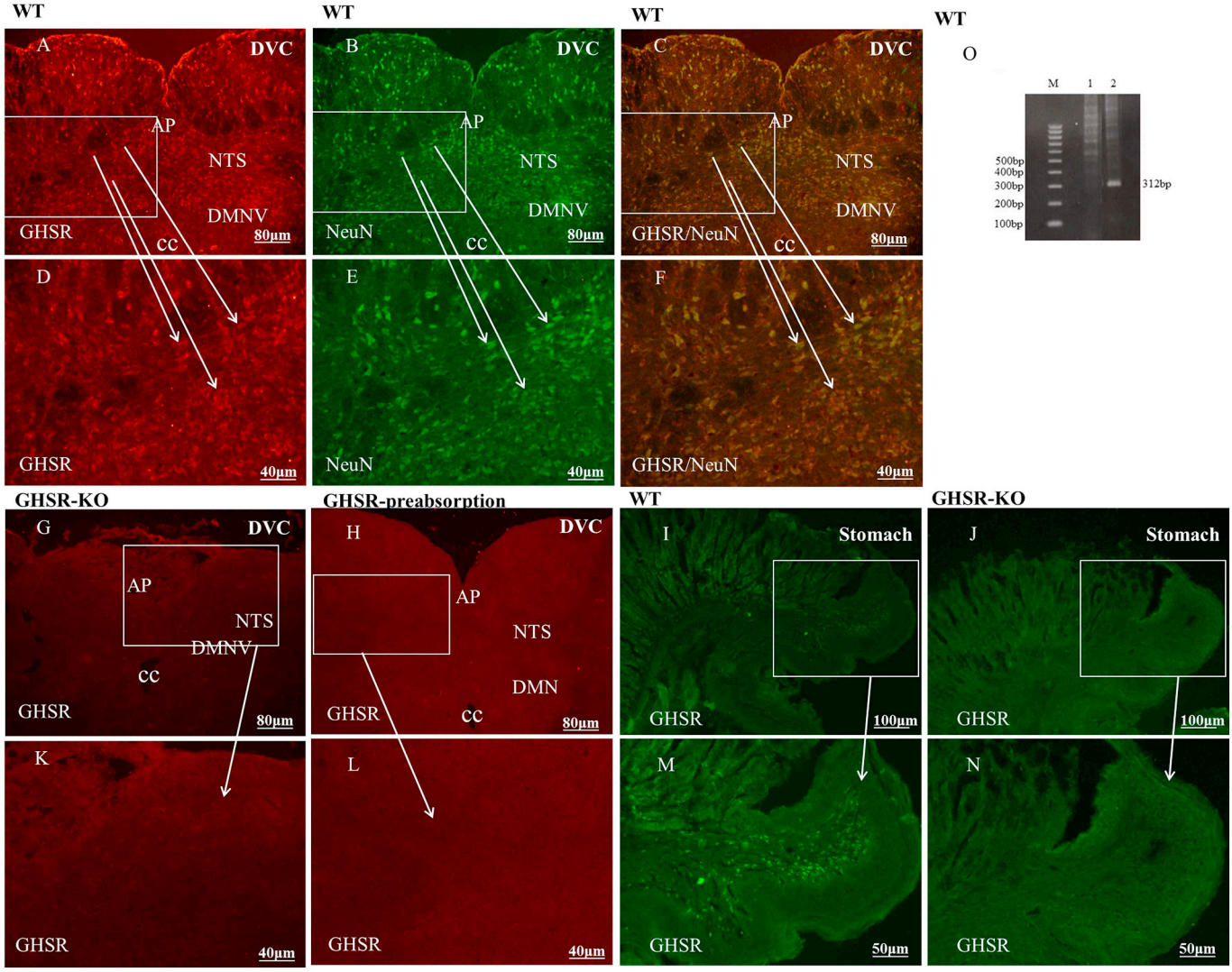

Fig. 2. Expression of GHSR-1a in the DVC in rats.
Fluorescent immunochemistry revealed GHSR-1a positive neurons in the DVC of the WT rats (A and D). NeuN staining localized to neurons in the DVC (B and E). Dual labeling of cells for both GHSR-1a and NeuN (C and F) indicated that the ghrelin receptor was expressed in the neurons, but not the astrocytes. There was no positive staining for GHSR-1a in the DVC of the GHSR-KO rats (G and K). The pre-absorption evaluation showed that immunoreactivity was destroyed by the GHSR protein (H and L). GHSR expression occurred in the gastric mucosa of the WT littermates (I and M), but no fluorescence signal was found in the GHSR-KO rats (J and N). As shown by the PCR assay, GHSR-1a, with a predicted band length of 312 bp, was detected in the DVC (O). WT: wild-type; AP: area postrema; NTS: nucleus tractus solitarius; DMNV: dorsal motor nucleus of the vagus; CC: central canal. M: markers; 1: loading buffer; 2: DVC. Scale bars, 80 μm or 40 μm; 100 μm or 50 μm.

charts. In all the analysis, a p value < .05 was considered statistically significant.

3. Results

3.1. The protein and mRNA expression of the ghrelin receptor GHSR-1a in the DVC

The protein and mRNA expression of GHSR-1a were determined using immunohistochemical and PCR methods, respectively. The GHSR-1a positive neurons were scattered in the DVC of the WT rats (Fig. 2A, D). The aforementioned finding was confirmed by a PCR assay, which demonstrated that GHSR-1a had a predicted band length of 312 bp (Fig. 2O). Staining for GHSR-1a and NeuN was performed simultaneously in the same slide (Fig. 2B, E). Dual labeling of cells for both GHSR-1a and NeuN (Fig. 2C, F) indicated that the ghrelin receptor was expressed in the neurons, but not in the astrocytes. To demonstrate the specificity of the antibodies, the expression of GHSR-1a was examined in the GHSR-KO rats. The results revealed no positive staining for GHSR-1a in the DVC of the GHSR-KO rats (Fig. 2G, K). The pre-absorption evaluation showed that immunoreactivity was destroyed by the GHSR protein (Fig. 2H, L). GHSR expression was found in the gastric mucosa of the WT littermates (Fig. 2I, M), but no fluorescence signal was found in the GHSR-KO rats (Fig. 2J, N).

3.2. Ghrelin fiber projections from the ARC to the DVC

After injecting FG into the DVC, FG-retrogradely-labeled neurons in the bilateral ARC were detected under a fluorescence microscope with ipsilateral side predominance (Fig. 3A, D). Ghrelin immunohistochemical staining on the same slide revealed ghrelin-immunopositive cells (Fig. 3B, E). Some ghrelin-immunopositive cells coexisted with the FG-fluorescently-labeled cells (Fig. 3C, F). Furthermore, scattered ghrelin immunoreactivity was observed in the ventromedial nucleus (Fig. 3C). Ghrelin expression was detected in the ghrelin-KO rats to verify specific staining for ghrelin immunoreactivity. The results revealed no positive staining for ghrelin in the ARC of the ghrelin-KO rats (Fig. 3G, K). The number of ghrelin-immunopositive

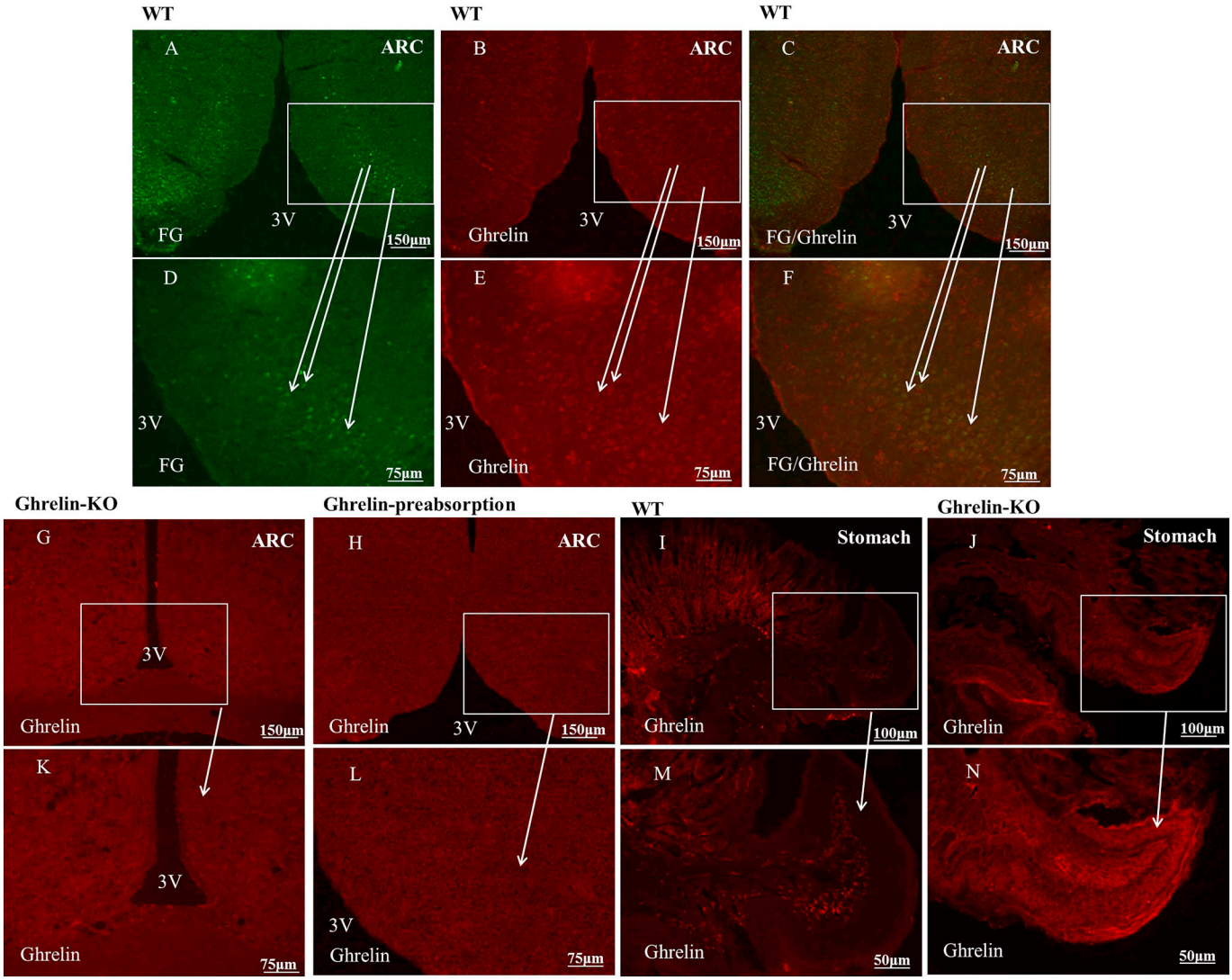

Fig. 3. Projection of ghrelin fibers from the ARC to the DVC.
After FG injection in the DVC, FG-labeled cells (A and D), ghrelin-immunopositive neurons (B and E), and double-labeled neurons (C and F) were found in the ARC. There was no positive staining for ghrelin in the ARC of the ghrelin-KO rats (G and K). The pre-absorption evaluation showed that immunoreactivity was destroyed by the ghrelin peptide (H and L). Ghrelin expression occurred in the gastric mucosa of the WT littermates (I and M), but no fluorescence signal was found in the ghrelin-KO rats (J and N). 3 V: third ventricle. Scale bars, 150 μm or 75 μm; 100 μm or 50 μm.

cells and FG-fluorescently-labeled cells in the ARC was 106.40 ± 5.18 cells and 52.20 ± 6.61 cells per field, respectively. Double-labeled cells accounted for 12.77 ± 2.69% of the ghrelin-immunopositive cells. The pre-absorption evaluation showed that immunoreactivity was destroyed by the ghrelin peptide (Fig. 3H, L). Ghrelin expression was seen in the gastric mucosa of the WT littermates (Fig. 3I, M), but no fluorescence signal was found in the ghrelin-KO rats (Fig. 3J, N).

3.3. The effects of ES of the ARC on ghrelin-responsive glucose-sensitive neurons in the DVC

A total of 220 neuron discharges were recorded in the DVC. Of these, 139 neurons were sensitive to glucose. Seventy-six (54.68%) neurons were GE and 63 (45.32%) were GI. After administering ghrelin in the DVC, 48 (63.16%) GE neurons were activated, with the firing frequency increasing from 4.46 ± 1.01 Hz to 6.83 ± 1.22 Hz (Fig. 4A, $p < .01$), and 42 (66.67%) GI neurons were inhibited, with the firing frequency decreasing from 4.39 ± 0.87 Hz to 2.07 ± 0.68 Hz (Fig. 4B, $p < .05$). These were identified as ghrelin-responsive GE or GI neurons. ES of the ARC excited the ghrelin-responsive GE and GI neurons, with the firing frequency increasing to 9.34 ± 2.05 Hz (Fig. 4A, $p < .01$) and 9.79 ± 2.13 Hz (Fig. 4B, $p < .01$), respectively. However, when the DVC was treated with the ghrelin receptor antagonist [D-Lys-3]-GHRP-6 prior to the ES of the ARC, the firing frequency of the ghrelin-responsive GE neurons (8.20 ± 1.09 Hz, Fig. 4A) and the GI neurons (8.66 ± 1.48 Hz, Fig. 4B) decreased significantly in comparison to those with ES only ($p < .05$). The firing frequency increased in comparison to the baseline discharge ($p < .01$), indicating a partial blockage effect of [D-Lys-3]-GHRP-6 in the DVC on the ES of the ARC.

3.4. The effects of ES of the ARC on glycolipid metabolism in rats

In the SS group, the serum glucose level decreased significantly 6 h after the SS (in comparison to 0 h, $p < .05$, Fig. 5E), but no change in the serum lipid parameters or insulin levels were observed (Fig. 5A–D, F). In the ES group, the serum TG, TC, and LDL-C levels increased, but the insulin level decreased 4 h after ES (in comparison to 0 h, $p < .05$ and $p < .01$, respectively; Fig. 5A–D, F), with a significant difference in these parameters, including serum glucose, in comparison to the SS group ($p < .05$ and $p < .01$, respectively; Fig. 5A–F). Six hours after

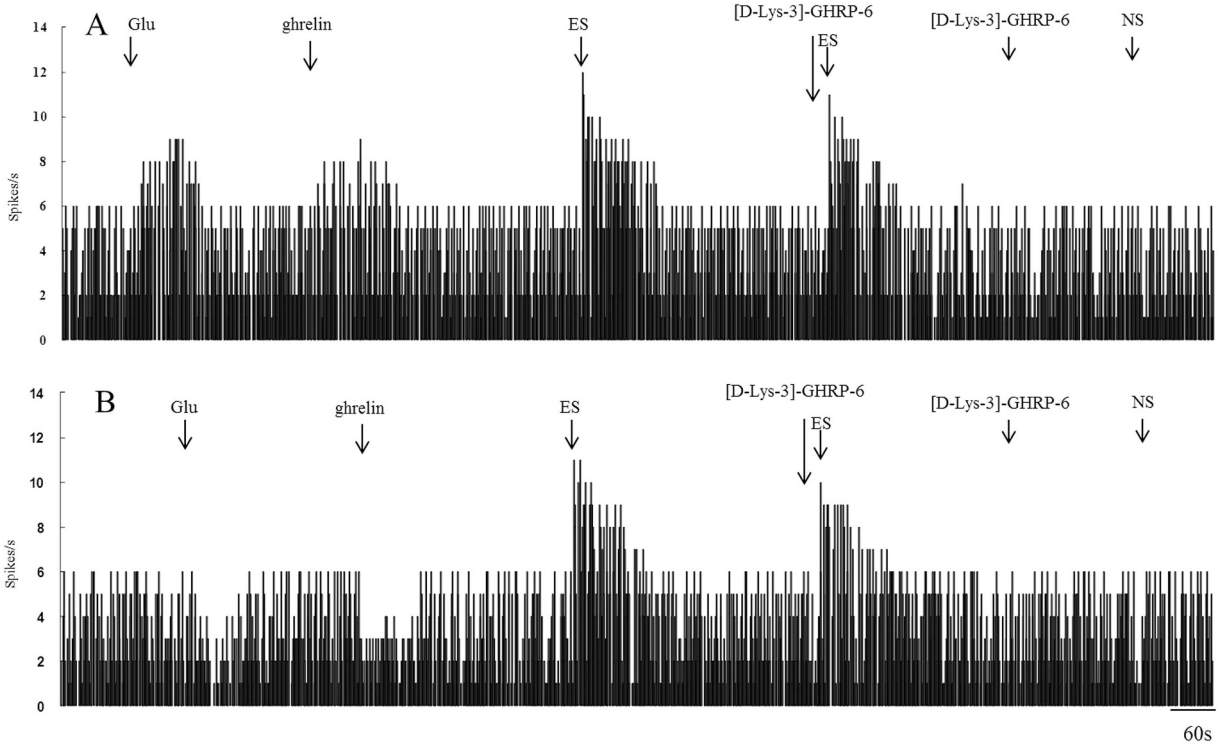

Fig. 4. Effects of ES of the ARC on ghrelin-responsive glucose-sensitive neurons in the DVC.
ES of the ARC excited ghrelin-responsive GE (A) or GI (B) neurons in the DVC; these effects were partially blocked by pretreatment with the ghrelin receptor antagonist [D-Lys-3]-GHRP-6 in the DVC.

ES, the above parameters changed significantly in comparison to 0 h, 2 h, and 4 h ($p < .05$ and $p < .01$, respectively, Fig. 5A–F). Therefore, 6 h after ES of the ARC was used as the observation time in subsequent experiments.

In comparison to the SS group, 6 h after ES of the ARC the following levels were elevated: serum TG (from 2.03 ± 0.31 mmol/L to 3.09 ± 0.56 mmol/L, $p < .01$, Fig. 6A), TC (from 0.39 ± 0.09 mmol/L to 0.64 ± 0.13 mmol/L, $p < .01$, Fig. 6B), LDL-C (from 0.76 ± 0.21 mmol/L to 1.74 ± 0.21 mmol/L, $p < .01$, Fig. 6C), and blood glucose (from 3.82 ± 0.84 mmol/L to 5.77 ± 1.17 mmol/L, $p < .01$, Fig. 6E). However, the following levels were decreased: serum HDL-C (from 1.86 ± 0.45 mmol/L to 1.22 ± 0.24 mmol/L, $p < .01$, Fig. 6D) and insulin (from 22.93 ± 5.22 mIU/L to 14.98 ± 2.39 mIU/L, $p < .01$, Fig. 6F). The blood lipid and glucose levels 6 h after ES of the VMH were also measured (Table 1); because there were only two cases, the data were not statistically analyzed. The effect of the ES of the VMH on the glycolipid metabolism might be explored in future research.

The serum TG (2.49 ± 0.28 mmol/L, Fig. 6A), TC (0.52 ± 0.10 mmol/L, Fig. 6B), LDL-C (1.29 ± 0.25 mmol/L, Fig. 6C), and blood glucose (4.86 ± 0.69 mmol/L, Fig. 6E) levels in the ES + [D-Lys-3]-GHRP-6 group decreased in comparison to the levels in the ES + NS group ($p < .05$ and $p < .01$, respectively); however, the levels were higher than those in the SS + [D-Lys-3]-GHRP-6 group ($p < .05$ and $p < .01$, respectively). The serum HDL-C (1.53 ± 0.31 mmol/L, Fig. 6D) and insulin (18.84 ± 3.71 mIU/L, Fig. 6F) levels in the ES + [D-Lys-3]-GHRP-6 group increased in comparison to the ES + NS group ($p < .05$ and $p < .01$, respectively), but they were lower than the levels in the SS + [D-Lys-3]-GHRP-6 group ($p < .05$). These results indicate that pre-administration of [D-Lys-3]-GHRP-6 in the DVC partially blocked ES-induced regulation of the circulating glucose and lipid levels in the ARC. The results obtained after pre-administration of BIM-28163 (Fig. 6A–F) in the DVC were similar to those obtained after pretreatment with [D-Lys-3]-GHRP-6 (Fig. 6A–F). These results provide further support for the involvement of the ghrelin-GHS-R system in ES-induced regulation of the circulating glucose and lipid levels in the ARC.

3.5. The effects of vagotomy on the serum biochemical parameters after ES of the ARC

The serum TG, TC, and LDL-C levels increased in the ES + sham group in comparison to the SS + sham group, but the HDL−C, glucose, and insulin levels decreased significantly ($p < .05$ and $p < .01$, respectively, Fig. 7A–F). A significant difference in the aforementioned biochemical parameters was observed in the ES + vago group in comparison to the ES + sham group; however, no significant difference was found between the ES + vago group and the SS + vago group. These findings indicated that vagotomy blocked the effects of ES of the ARC on glycolipid metabolism.

3.6. The effects of ES of the ARC on the expression of liver enzymes

Six hours after ES of the ARC, the hepatic ACC-1 levels increased significantly in the ES + [D-Lys-3]-GHRP-6 group in comparison to the SS group, from 0.79 ± 0.08 to 1.35 ± 0.16 ($p < .01$, Fig. 8A), and the hepatic CPT-1 levels decreased significantly, from 0.42 ± 0.05 to 0.23 ± 0.03 ($p < .01$, Fig. 8B). The hepatic ACC-1 levels decreased in the ES + [D-Lys-3]-GHRP-6 group (1.23 ± 0.13) in comparison to the ES + NS group (1.41 ± 0.19, $p < .05$, Fig. 8A), but they were higher than those in the SS + [D-Lys-3]-GHRP-6 group (0.68 ± 0.07, $p < .01$, Fig. 8A). The hepatic CPT-1 levels increased in the ES + [D-Lys-3]-GHRP-6 group (0.33 ± 0.05) in comparison to the ES + NS group (0.21 ± 0.02, $p < .01$, Fig. 8B), but they were lower than those in the SS + [D-Lys-3]-GHRP-6 group (0.39 ± 0.06, $p < .05$, Fig. 8B). These results indicate that pre-administration of [D-Lys-3]-GHRP-6 in the DVC partially blocked the effects of ES of the ARC on lipid metabolism in the liver.

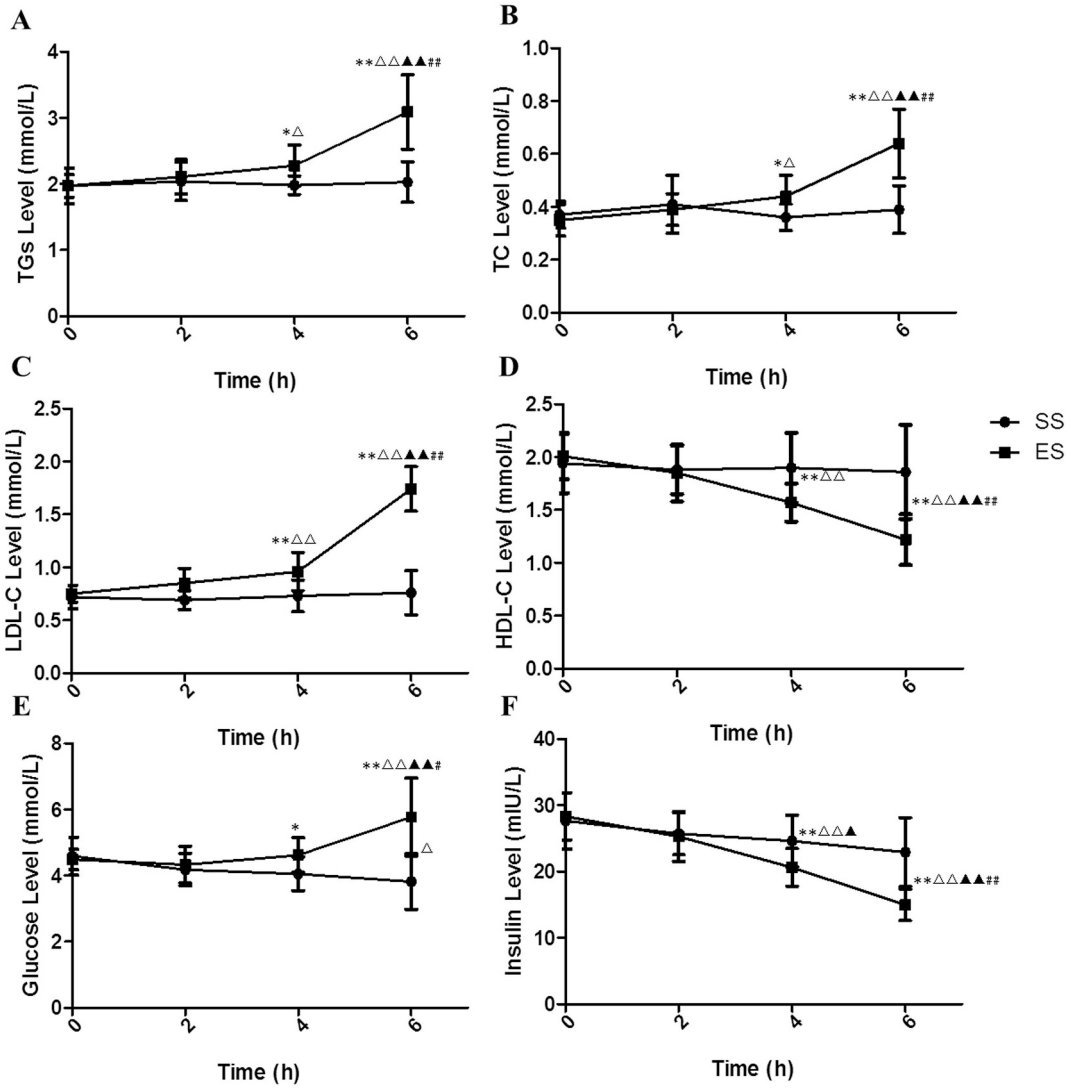

Fig. 5. Changes in the blood biochemical parameters 0–6 h after ES of the ARC.
In the SS group, the serum glucose level decreased significantly 6 h after SS (E). In the ES group, the serum TG, TC, and LDL-C levels increased, but the insulin levels decreased 4 h after ES (A–D, F). A significant difference was found in the levels of these parameters, including serum glucose levels, in the ES group in comparison to the SS group (A–F). Six hours after ES, the aforementioned biochemical parameters changed significantly (A–F). TG: triglyceride (A); TC: total cholesterol (B); LDL-C: low-density lipoprotein cholesterol (C); HDL—C: high-density lipoprotein cholesterol (D); glucose (E); insulin (F). In comparison to the SS group, $^{*}p < .05$, $^{**}p < .01$. In comparison to 0 h, $^{\triangle}p < .05$, $^{\triangle\triangle}p < .01$. In comparison to 2 h, $^{\blacktriangle}p < .05$, $^{\blacktriangle\blacktriangle}p < .01$. In comparison to 4 h, $^{\#}p < .05$, $^{\#\#}p < .01$.

3.7. The effects of ES of the ARC on the expression of AgRP/NPY in the ARC and ghrelin in the DVC

Six hours after ES of the ARC, the protein expression of AgRP and NPY increased significantly in the ARC, from 0.32 ± 0.11 to 0.82 ± 0.26 ($p < .01$) and from 0.48 ± 0.17 to 0.89 ± 0.38 ($p < .05$), respectively (Fig. 9A, B). Furthermore, the expression of ghrelin in the DVC increased significantly, from 0.19 ± 0.04 to 0.36 ± 0.11 ($p < .05$, Fig. 9A, B). These results demonstrate that ES of the ARC can increase the level of AgRP/NPY and stimulate ghrelin expression in the DVC.

4. Discussion

This study investigated the ghrelin neural pathway from the ARC to the DVC and the effects of this pathway on glycolipid metabolism in rats. The results indicate that ghrelin neurons in the ARC were projected into the DVC. Moreover, protein expression and mRNA expression of GHSR-1a were observed in the DVC neurons. ES of the ARC regulated the discharge of ghrelin-responsive glucose-sensitive neurons in the DVC and significantly promoted glycolipid metabolism in rats, but this effect was partially blocked by pre-administration of [D-Lys-3]-GHRP-6 in the DVC. Based on these findings, the ghrelin neural pathway from the ARC to the DVC could possibly participate in the integration of glucose metabolic signal transmission to regulate glycolipid metabolism.

The hypothalamus is involved in the regulation of various metabolic processes and autonomic nervous system activities, including body temperature, hunger, thirst, fatigue, sleep, and circadian rhythms, and the ARC is an important site to integrate these signals. A recent study provided direct evidence that ghrelin was expressed in the ARC (Guan et al., 2008). Intriguingly, the ghrelin receptor was expressed adjacent to where the ghrelin gene was expressed. A number of studies have confirmed that extensive fiber connections between the ARC, paraventricular nucleus (PVN), ventromedial nucleus, and DVC are involved in feeding and gastric motility regulation (Bouret et al., 2004; Bouyer and Simerly, 2013; Wilson and Enriori, 2015; Luan et al., 2017). It is not known whether there are projections of ghrelin fibers in these

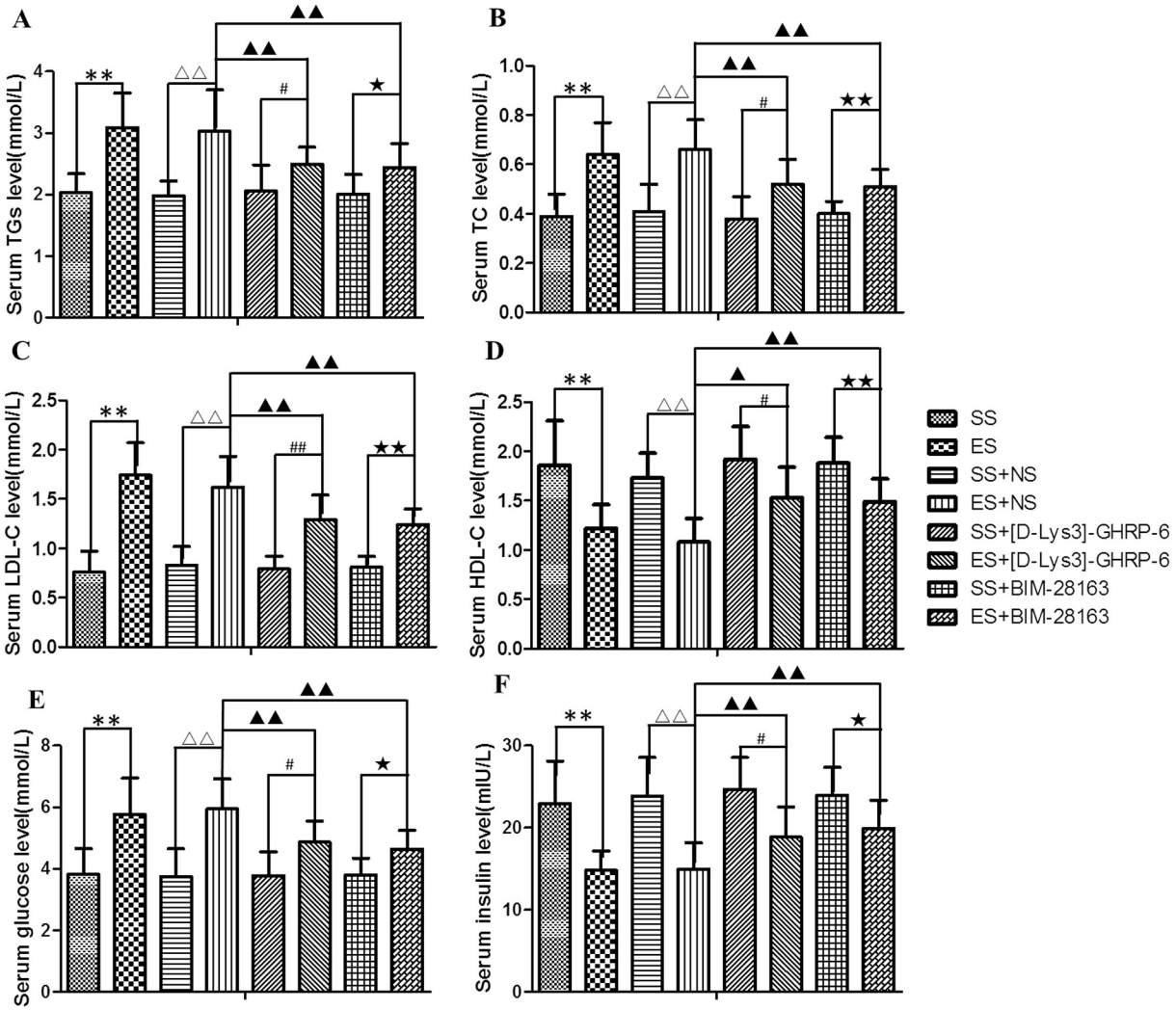

Fig. 6. Effects of ES of the ARC on glycolipid metabolism.
Six hours after ES of the ARC, the serum TG, TC, LDL-C, and glucose levels increased, but the HDL-C and insulin levels decreased; these effects were partially blocked by pretreatment with [D-Lys-3]-GHRP-6 or BIM-28163 in the DVC prior to ES. TG: triglyceride (A); TC: total cholesterol (B); LDL-C: low-density lipoprotein cholesterol (C); HDL−C: high-density lipoprotein cholesterol (D); glucose (E); insulin (F). In comparison to the SS group, $^{*}p < .05$, $^{**}p < .01$. In comparison to the SS + NS group, $^{\triangle}p < .05$, $^{\triangle\triangle}p < .01$. In comparison to the SS + [D-Lys-3]-GHRP group, $^{\#}p < .05$, $^{\#\#}p < .01$. In comparison to the ES + NS group, $^{\blacktriangle}p < .05$, $^{\blacktriangle\blacktriangle}p < .01$. In comparison to the SS + BIM-28613 group, $^{\star}p < .05$, $^{\star\star}p < .01$.

Table 1
Data of the serum biochemical parameters after ES of the VMH.

Sample	1	2
TGs (mmol/L)	2.21	2.33
TC (mmol/L)	0.47	0.42
LDL-C (mmol/L)	1.06	1.13
HDL-C (mmol/L)	1.89	1.76
Glucose (mmol/L)	4.32	4.29
Insulin (mIU/L)	20.07	18.36

neural pathways.

For the past five years, our research group has investigated the ghrelin neural pathway in the hypothalamus and other brain areas (Gong et al., 2014; Gong et al., 2017a; Gong et al., 2017b; Liu et al., 2019). Based on the present study's findings, ghrelin fibers project from the ARC into the DVC. The latter was confirmed by neuron retrograde tracking, combined with fluorescent immunohistochemistry. The expression of the ghrelin receptor GHSR-1a in DVC neurons suggests that this neural pathway plays a regulatory role via biding to its receptor. A previous immunohistochemical analysis revealed that the ghrelin receptor was expressed in the NTS and DMNV, but not in cells in the AP (Lin et al., 2004). Ghrelin receptor mRNA and immunoreactivity were detected in the DMNV (Zhang et al., 2004) and was highly expressed in the NTS (Cornejo et al., 2018). Another study reported GHSR-1a mRNA expression in all the components of the DVC, with the highest expression in the AP, a moderately dense signal in the NTS, and a low-density signal in the DMNV (Zigman et al., 2006). The experimental results of the present study revealed GHSR-1a expression throughout the DVC and high expression in the NTS. The absence of positive staining for GHSR-1a in the DVC of GHSR-KO rats confirmed these results.

Hypothalamic ARC is an important target for the orexigenic and energy homeostatic effects of ghrelin through NPY- and AgRP-expressing neurons (Kageyama et al., 2010; Lv et al., 2018), and glucose-sensing neurons within this region respond to ghrelin (Chen et al., 2005). The present study revealed that the ghrelin neuronal pathway arose in the ARC and projected into the DVC. Recently, there has been debate about whether ghrelin is produced in the hypothalamus. Some studies have concluded that substantial secretion of ghrelin from the ARC was unlikely (Edwards and Abizaid, 2017; Furness et al., 2011). However, other studies identified ghrelin expression in the central nervous system using various methods, including reversed-phase high-

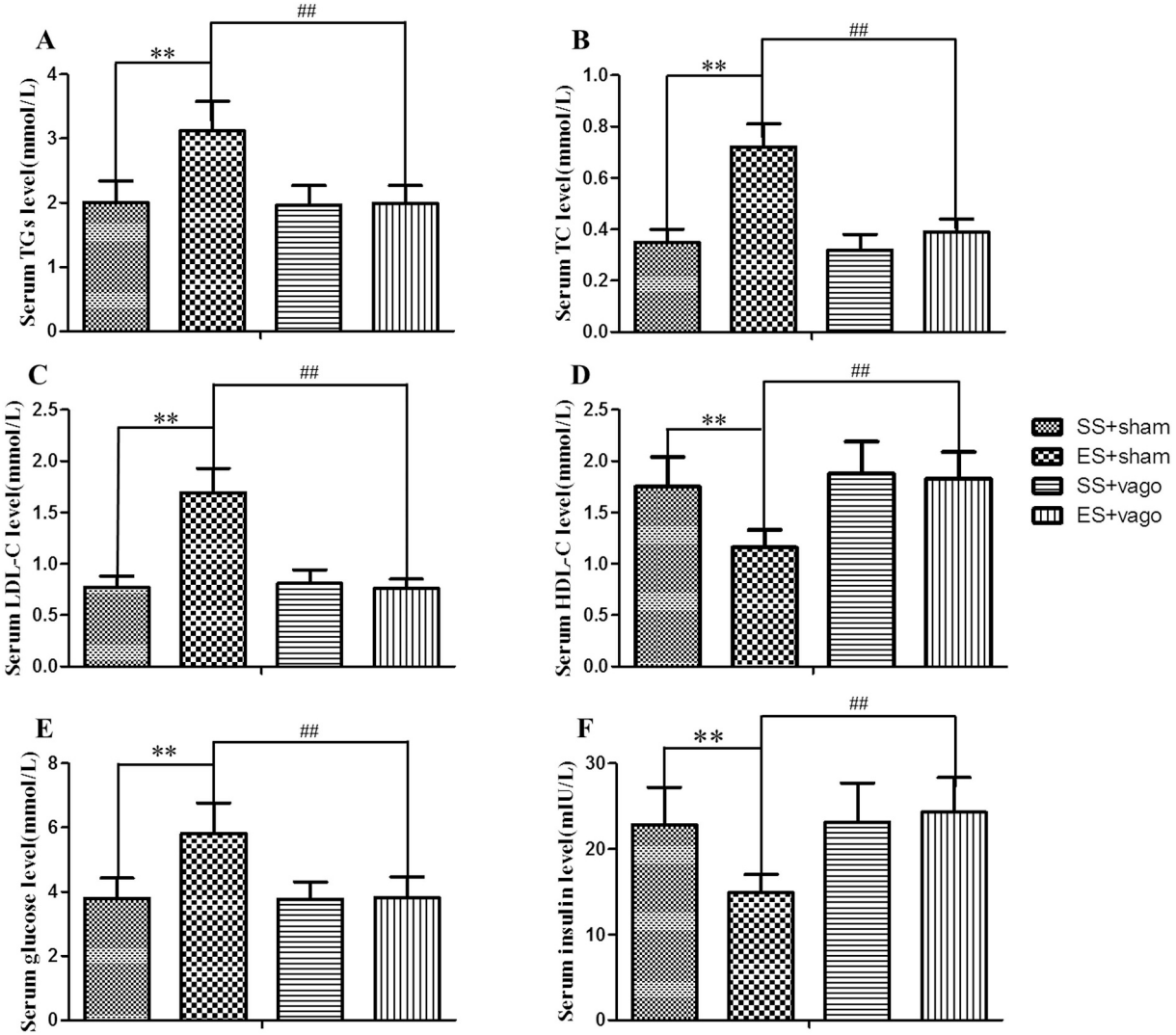

Fig. 7. Effects of vagotomy on the serum biochemical parameters after ES of the ARC.
The serum TG, TC, and LDL-C levels increased, but the HDL−C, glucose, and insulin levels decreased significantly in the ES + sham group (A–F). A significant difference was found in these biochemical parameters in the ES + vago group in comparison to the ES + sham group, but no significant difference was found in comparison to the SS + vago group (A–F). TG: triglyceride (A); TC: total cholesterol (B); LDL-C: low-density lipoprotein cholesterol (C); HDL−C: high-density lipoprotein cholesterol (D); glucose (E); insulin (F). In comparison to the SS + sham group, $^{*}p < .05$, $^{**}p < .01$. In comparison to the ES + sham group, $^{\#}p < .05$, $^{\#\#}p < .01$.

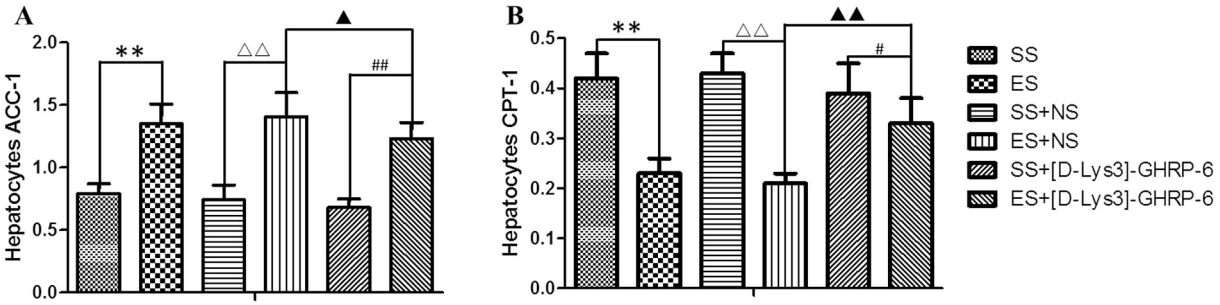

Fig. 8. Effects of ES of the ARC on the expression of liver enzymes.
Six hours after ES of the ARC, the hepatic ACC-1 levels (A) were significantly elevated, but the hepatic CPT-1 levels (B) were significantly reduced; these effects were partially blocked by pre-administration of [D-Lys-3]-GHRP-6 in the DVC. ACC-1: acetyl-CoA carboxylase-1 (A); CPT-1: carnitine palmitoyltransferase-1 (B). In comparison to the SS group, $^{*}p < .05$, $^{**}p < .01$. In comparison to the SS + NS group, $^{\triangle}p < .05$, $^{\triangle\triangle}p < .01$. In comparison to the SS + [D-Lys-3]-GHRP group, $^{\#}p < .05$, $^{\#\#}p < .01$. In comparison to the ES + NS group, $^{\blacktriangle}p < .05$, $^{\blacktriangle\blacktriangle}p < .01$.

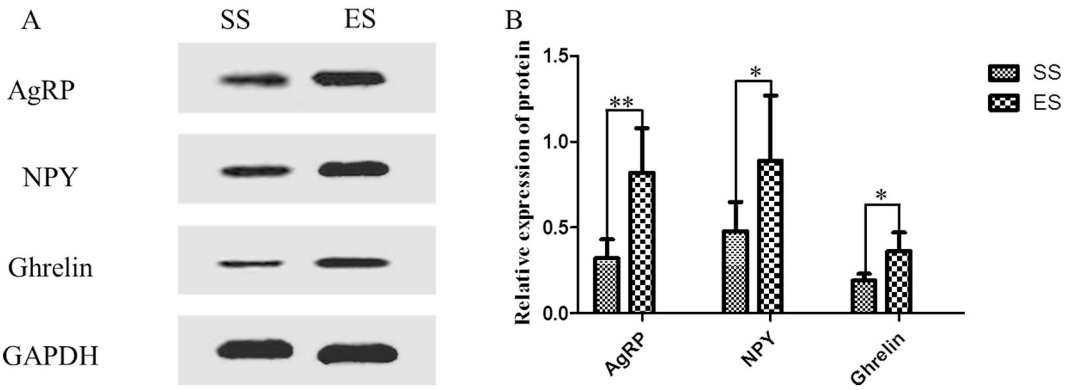

Fig. 9. Effects of ES of the ARC on the expression of AgRP/NPY in the ARC and ghrelin in the DVC.
Six hours after ES of the ARC, the expression of AgRP and NPY in the ARC and ghrelin in the DVC significantly increased (A and B). AgRP: agouti-related protein; NPY: neuropeptide Y; GAPDH: glyceraldehyde-3-phosphate dehydrogenase. In comparison to the SS group, $*p < .05$, $**p < .01$.

performance liquid chromatography (RP-HPLC) combined with C-radioimmunoassay (C-RIA) (Hosoda et al., 2000; Sato et al., 2005), RP-HPLC combined with N- radioimmunoassay (N-RIA) (Mondal et al., 2005), ELISAs (Furness et al., 2011; Ergul Erkec et al., 2018), PCR methods (Lv et al., 2016), immunohistochemistry (Cui et al., 2014; Lv et al., 2016; Russo et al., 2017a; Russo et al., 2017b), and Western blotting (Cui et al., 2014; Huang et al., 2011). A recent report revealed the presence of ghrelin-O-acyltransferase (GOAT) and its ability to acylate non-octanoylated ghrelin in the hippocampus (Murtuza and Isokawa, 2017). The differences in the findings from these studies may be primarily related to differences in the specificities of the detection methods, the types of ghrelin antibodies used, and individual differences in the rats. To verify specific staining for ghrelin, in the present study the expression of ghrelin in the ghrelin-KO rats was detected. The results revealed no positive staining for ghrelin in the ARC and stomachs of the ghrelin-KO rats.

Ghrelin binding to GHSR-1a elicits an orexigenic response through enhanced expression of AgRP/NPY and decreased expression of proopiomelanocortin (Velásquez et al., 2011). This orexigenic effect is mediated by changes in fatty acid metabolism and other parameters related to fatty acid-sensing systems (López et al., 2008; Sangiao-Alvarellos et al., 2010; Martins et al., 2013; Gao et al., 2013; Stark et al., 2015). In a previous study, exogenous ghrelin, unilaterally microinjected into the DVC, increased food intake when combined with GHSR (Faulconbridge et al., 2003). Ghrelin administration into the DVC induced a hyperphagic effect, which was involved in the activation of NPY/AgRP neurons in the ARC (Guan et al., 2010). In the present study, ES of the ARC increased the ARC expression of AgRP and NPY, suggesting that NPY/AgRP neurons in the ARC may participate in glycolipid metabolism (Zagmutt et al., 2018). However, selective GHSR expression in the hindbrain was not found to be sufficient for restoring ghrelin-stimulated food intake (Scott et al., 2012). In one study, decreased fasting blood glucose levels, observed in the GHSR-KO mice, returned to WT levels by selective re-expression of hindbrain GHSR, indicating that ghrelin has a role in the regulation of glucose metabolism (Scott et al., 2012). In the present study, GHSR-1a expression in the GHSR-KO rats was detected using specific staining for GHSR-1a. The results revealed no positive staining for GHSR-1a, both in the DVC and the stomachs of the GHSR-KO rats. To elucidate this, the present study investigated the role of the ghrelin neural pathway in glycolipid metabolism via binding to its receptor in the DVC.

The maintenance of glucose homeostasis depends on the ability of the central nervous system and the peripheral tissues to sense changes in glucose levels. Preprandial and fasting-induced increases in circulating ghrelin (Van et al., 2004; Spiegel et al., 2011; Zhao et al., 2010), and hypothalamic GHSR gene expression (Kim et al., 2003) pointed to the involvement of a central mechanism, whereby the ghrelin system can sense declining glucose levels (Sun et al., 2007). Glucose-sensitive neurons in the brain respond to changes in extracellular glucose and regulate glucose homeostasis (Routh, 2002). In the present study, the discharge of glucose-sensitive neurons (GE and GI neurons) in the DVC were recorded. Interestingly, these neurons were responsive to ghrelin microinjected into the DVC. To elucidate the ghrelin neural pathway from the ARC to the DVC, discharges from these neurons were observed following ES of the ARC. The results revealed that ES of the ARC excited the ghrelin-responsive GE and GI neurons. These effects were partially blocked by pre-administration of [D-Lys-3]-GHRP-6 in the DVC, thus implying that the ghrelin neural pathway from the ARC to the DVC sensed glucose-sensing afferent signals from the peripheral circulation. Consequently, efferent signals were sent to the periphery via the vagus nerve to adjust glycolipid metabolism.

To elucidate the regulation of the ghrelin neural pathway on glycolipid metabolism, the effects of ES of the ARC on circulating glucose and lipid levels were observed. The results showed that ES of the ARC significantly elevated the serum TG, TC, LDL-C, and glucose levels and reduced the HDL-C and insulin levels, and these effects were partially blocked by pre-administration of [D-Lys-3]-GHRP-6 or BIM-28163 in the DVC. Ghrelin expression in the DVC increased significantly after stimulation of the ARC, thus indicating that ghrelin was released by stimulation of the ARC and transported to the DVC. Furthermore, the ghrelin receptor antagonist partly blocked the effect of ARC stimulation on the regulation of glucose-sensitive neuron discharges and glycolipid metabolism, which further verified that ghrelin was a neurotransmitter released by the ARC. Combined with ghrelin fiber projection from the ARC to the DVC, it can be speculated that ghrelin is released by stimulation of the ARC and that ghrelin projections from the ARC to the DVC regulate glucose-sensing afferent signals and glycolipid metabolism.

In addition to the regulation of appetite and growth hormone secretion, ghrelin enhances autophagy by activating AMP-activated protein kinases in different target organs to improve remodeling and protection of small intestinal mucosa, prevent myocardial ischemia, improve brain function (e.g., learning and memory consolidation), and regulate lipid and glucose metabolism (Müller et al., 2015; Churm et al., 2017). Recently, the role of ghrelin in the regulation of lipid and glucose metabolism has received a significant amount of research attention because pharmacological inhibition of ghrelin signaling may have therapeutic value for improving insulin resistance and treating type 2 diabetes (Ahmed et al., 2017). To date, several studies have pointed to a negative correlation between ghrelin levels and the incidence of type 2 diabetes and insulin resistance (Ikezaki et al., 2002; Broglio et al., 2003; Poykko et al., 2003; Katsuki et al., 2004). In the present study, the finding of a ghrelin neural pathway from the ARC to the DVC highlights that it may be related to glucose and lipid metabolism.

In the present study, vagotomy eliminated the regulatory effect of ES of the ARC on glycolipid metabolism, resulting in the involvement of the vagus nerve in afferent signal regulation. To explore the fundamental mechanism of the ghrelin neural pathway from the ARC to the DVC in the regulation of lipid metabolism, the effect of ES of the ARC on liver ACC-1 and CPT-1 expression was detected. ACC-1 provides a malonyl-CoA substrate for the biosynthesis of fatty acids. CPT-1 catalyzes the conversion of long-chain fatty acyl-CoA into acylcarnitines, which is the first step in the transport of long-chain fatty acids from the cytoplasm to the mitochondrial matrix, where they undergo β-oxidation (Gao et al., 2013). ES of the ARC increased ACC-1 expression and decreased CPT-1 expression in the liver, pointing to promotion of cholesterol synthesis and inhibition of β-oxidation, which resulted in lipid accumulation. The partial blockage of ES in the ARC on the expression of liver enzymes by the ghrelin receptor antagonist implied that the ghrelin neural pathway from the ARC to the DVC regulated lipid metabolism via the ghrelin receptor in the DVC. Further studies are needed to support these findings.

In conclusion, the study's results suggest that the ghrelin neural pathway from the ARC to the DVC plays a role in glycolipid metabolism via the GHSR-1a receptor in the DVC. The detailed mechanisms underlying ghrelin-induced regulation of glycolipid metabolism must still be investigated.

Funding

This work was supported by the Shandong Key Research and Development Program (Project No. 2018GSF119005), National Training Program of Innovation and Entrepreneurship for Undergraduates (Project No: 201810426025), the Eco-chemical Engineering Cooperative Innovation Center of Shandong, and the Shandong Key Lab of Multiphase Fluid Reaction & Separation Engineering.

Declaration of Competing Interest

None.

Acknowledgments

The experiments were performed in the pharmacy laboratory at Qingdao University of Science and Technology. We would like to express our sincere gratitude to Dr. Xu Luo and Dr. Sun Xiangrong for their support and technical guidance during the experiments. We would also like to thank Dr. Guo Feifei and Dr. Luan Xiao for providing the experimental instruments. Finally, we would like to thank our colleagues for their invaluable assistance in the preparation of this manuscript.

References

Ahmed, A.Q.A., Elbahi, J.F., Nagalla, D., Mohamed, A., Mona, E., Gasim, A.Z.A., Muhalab, E.A., Abdulaziz, A.M., Abdirashid, M.S., Khalid, G., Hayder, A.G., 2017. Association of plasma ghrelin levels with insulin resistance in type 2 diabetes mellitus among saudi subjects. Endocrinol. Metab. 32 (2), 230–240. https://doi.org/10.3803/EnM.2017.32.2.230.

Babic, T., Browning, K.N., 2014. The role of vagal neurocircuits in the regulation of nausea and vomiting. Eur. J. Pharmacol. 722 (1433), 38–47. https://doi.org/10.1016/j.ejphar.2013.08.047.

Blouet, C., Schwartz, G.J., 2010. Hypothalamic nutrient sensing in the control of energy homeostasis. Behav. Brain Res. 209 (1), 1–12. https://doi.org/10.1016/j.bbr.2009.12.024.

Bouret, S.G., Draper, S.J., Simerly, R.B., 2004. Formation of projection pathways from the Arcuate nucleus of the hypothalamus to hypothalamic regions implicated in the neural control of feeding behavior in mice. J. Neurosci. 24 (11), 2797–2805. https://doi.org/10.1523/JNEUROSCI.5369-03.2004.

Bouyer, K., Simerly, R.B., 2013. Neonatal Leptin exposure specifies innervation of Presympathetic hypothalamic neurons and improves the metabolic status of Leptin deficient mice. J. Neurosci. 33 (2), 840–851. https://doi.org/10.1523/JNEUROSCI.3215-12.2013.

Broglio, F., Gottero, C., Benso, A., Prodam, F., Volante, M., Destefanis, S., Gauna, C., Muccioli, G., Papotti, M., van der Lely, A.J., Ghigo, E., 2003. Ghrelin and the endocrine pancreas. Endocrine 22 (1), 19–24. https://doi.org/10.1385/ENDO:22:1:19.

Cahill, S.P., Hatchard, T., Abizaid, A., Holahan, M.R., 2014. An examination of early neural and cognitive alterations in hippocampal-spatial function of ghrelin receptor-deficient rats. Behav. Brain Res. 264, 105–115. https://doi.org/10.1016/j.bbr.2014.02.004.

Chen, X., Ge, Y., Jiang, Z.Y., Liu, C.Q., Depoortere, I., Peeters, T.L., 2005. Effects of ghrelin on hypothalamic glucose responding neurons in rats. Brain Res. 1055 (1), 131–136. https://doi.org/10.1016/j.brainres.2005.06.080.

Churm, R., Davies, J.S., Stephens, J.W., Prior, S.L., 2017. Ghrelin function in human obesity and type 2 diabetes: a concise review. Obes. Rev. 18 (2), 140–148. https://doi.org/10.1111/obr.12474.

Colldén, G., Tschöp, M.H., Müller, T.D., 2017. Therapeutic potential of targeting the ghrelin pathway. Int. J. Mol. Sci. 18 (4), 798. https://doi.org/10.3390/ijms18040798.

Cornejo, M.P., Francesco, P.N.D., Romero, G.G., Portiansky, E.L., Zigman, J.M., Reynaldo, M., Perello, M., 2018. Ghrelin receptor signaling targets segregated clusters of neurons within the nucleus of the so litary tract. Brain Struct. Funct. 223 (7), 3133–3147. https://doi.org/10.1007/s00429-018-1682-5.

Cui, L.L., Li, P., Zhu, Z.Y., 2014. Impact of changes in postnatal nutrition on puberty onset and the expression of hypothalamic GnRH and ghrelin. Eur. Rev. Med. Pharmacol. Sci. 18 (5), 703–709.

Delhanty, P.J., Van, d.L., 2011. Ghrelin and glucose homeostasis. Peptides 32 (11), 2309–2318. https://doi.org/10.1016/j.peptides.2011.03.001.

Diéguez, C., Frühbeck, G., López, M., 2009. Hypothalamic lipids and the regulation of energy homeostasis. Obesity Facts 2 (2), 126–135. https://doi.org/10.1159/000209251.

Edwards, A. and Abizaid, A., 2017. Clarifying the ghrelin system's ability to regulate feeding behaviours despite enigmatic spatial separation of the GHSR and its endogenous ligand. Int. J. Mol. Sci., 18(4). https://www.mdpi.com/1422-0067/18/4/859

Ergul Erkec, O., Algul, S., Kara, M., 2018. Evaluation of ghrelin, nesfatin-1 and irisin levels of serum and brain after acute or chronic pentylenetetrazole administrations in rats using sodium valproate. Neurol. Res. 40 (11), 923–929. https://doi.org/10.1080/01616412.2018.1503992.

Faulconbridge, L.F., Cummings, D.E., Kaplan, J.M., Grill, H.J., 2003. Hyperphagic effects of brainstem ghrelin administration. Diabetes 52 (9), 2260–2265. https://doi.org/10.2337/diabetes.52.9.2260.

Folmes, C.D.L., Lopaschuk, G.D., 2007. Role of malonyl-CoA in heart disease and the hypothalamic control of obesity. Cardiovasc. Res. 73 (2), 278–287. https://doi.org/10.1016/j.cardiores.2006.10.008.

Furness, J.B., Hunne, B., Matsuda, N., Yin, L., Russo, D., Kato, I., Fujimiya, M., Patterson, M., McLeod, J., Andrews, Z.B., Bron, R., 2011. Investigation of the presence of ghrelin in the central nervous system of the rat and mouse. Neuroscience 193, 1–9. https://doi.org/10.1016/j.neuroscience.2011.07.063.

Gao, S., Casals, N., Keung, W., Moran, T.H., Lopaschuk, G.D., 2013. Differential effects of central ghrelin on fatty acid metabolism in hypothalamic ventral medial and arcuate nuclei. Physiol. Behav. 118, 165–170. https://doi.org/10.1016/j.physbeh.2013.03.030.

Gong, Y., Xu, L., Guo, F., Pang, M., Shi, Z., Gao, S., Sun, X., 2014. Effects of ghrelin on gastric distension sensitive neurons and gastric motility in the lateral septum and arcuate nucleus regulation. J. Gastroenterol. 49 (2), 219–230. https://doi.org/10.1007/s00535-013-0789-y.

Gong, Y., Liu, Y., Liu, F., Wang, S., Jin, H., Guo, F., Xu, L., 2017a. Ghrelin fibers from lateral hypothalamus project to nucleus tractus solitaries and are involved in gastric motility regulation in cisplatin-treated rats. Brain Res. 1659, 29–40. https://doi.org/10.1016/j.brainres.2017.01.004.

Gong, Y., Liu, Y., Guo, Y., Su, M., Zhong, Y., Xu, L., Guo, F., Gao, S., 2017b. Ghrelin projection from the lateral hypothalamus area to the dorsal vagal complex and its regulation of gastric motility in cisplatin-treated rats. Neuropeptides 66, 69–80. https://doi.org/10.1016/j.npep.2017.09.003.

Guan, J.L., Okuda, H., Takenoya, F., Kintaka, Y., Yagi, M., Wang, L., Seki, M., Hori, Y., Kageyama, H., Shioda, S., 2008. Synaptic relationships between proopiomelanocortin- and ghrelin-containing neurons in the rat arcuate nucleus. Regul. Pept. 145 (1–3), 128–132. https://doi.org/10.1016/j.regpep.2007.09.028.

Guan, H.Z., Li, Q.C., Jiang, Z.Y., 2010. Ghrelin acts on rat dorsal vagal complex to stimulate feeding via arcuate neuropeptide Y/agouti-related peptide neurons activation. Shen Li Xue Bao 62 (4), 357–364.

Hosoda, H., Kojima, M., Matsuo, H., Kangawa, K., 2000. Ghrelin and des-acyl ghrelin: two major forms of rat ghrelin peptide in gastrointestinal tissue. Biochem. Biophys. Res. Commun. 279 (3), 909–913. https://doi.org/10.1006/bbrc.2000.4039.

Huang, L., Qiu, B., Yuan, L., Zheng, L., Li, Q., Zhu, S., 2011. Influence of fasting, insulin and glucose on ghrelin in the dorsal vagal complex in rats. J. Endocrinol. 211 (3), 257–262. https://doi.org/10.1530/JOE-11-0147.

Ikezaki, A., Hosoda, H., Ito, K., Iwama, S., Miura, N., Matsuoka, H., Kondo, C., Kojima, M., Kangawa, K., Sugihara, S., 2002. Fasting plasma ghrelin levels are negatively correlated with insulin resistance and pai-1, but not with leptin, in obese children and adolescents. Diabetes 51 (12), 3408–3411. https://doi.org/10.2337/diabetes.51.12.3408.

Kageyama, H., Takenoya, F., Shiba, K., Shioda, S., 2010. Neuronal circuits involving ghrelin in the hypothalamus-mediated regulation of feeding. Neuropeptides 44 (2), 133–138. https://doi.org/10.1016/j.npep.2009.11.010.

Katsuki, A., Urakawa, H., Gabazza, E.C., Murashima, S., Nakatani, K., Togashi, K., Yano, Y., Adachi, Y., Sumida, Y., 2004. Circulating levels of active ghrelin is associated with abdominal adiposity, hyperinsulinemia and insulin resistance in patients with type 2

diabetes mellitus. Eur. J. Endocrinol. 151 (5), 573–577. https://doi.org/10.1530/eje.0.1510573.
Kim, M.S., Yoon, C.Y., Park, K.H., Shin, C.S., Park, K.S., Kim, S.Y., Cho, B.Y., Lee, H.K., 2003. Changes in ghrelin and ghrelin receptor expression according to feeding status. Neuroreport 14 (10), 1317–1320. https://doi.org/10.1097/01.wnr.0000078703.79393.d2.
Le Foll, C., Irani, B.G., Magnan, C., Dunn-Meynell, A.A., Levin, B.E., 2009. Characteristics and mechanisms of hypothalamic neuronal fatty acid sensing. Am. J. Phys. Regul. Integr. Comp. Phys. 297 (3), 655–664. https://doi.org/10.1152/ajpregu.00223.2009.
Lin, Y., Matsumura, K., Fukuhara, M., Kagiyama, S., Fujii, K., Iida, M., 2004. Ghrelin acts at the nucleus of the solitary tract to decrease arterial pressure in rats. Hypertension 43 (5), 977–982. https://doi.org/10.1161/01.HYP.0000122803.91559.55.
Liu, Y., Yan, M., Guo, Y., Niu, Z., Sun, R., Jin, H., Gong, Y., 2019. Ghrelin and electrical stimulating the lateral hypothalamus area regulated the discharges of gastric distention neurons via the dorsal vagal complex in cisplatin-treated rats. Gen. Comp. Endocrinol. 279, 174–183. https://doi.org/10.1016/j.ygcen.2019.03.014.
López, M., Lage, R., Saha, A.K., Pérez-Tilve, D., Vázquez, M.J., Varela, L., Sangiao-Alvarellos, S., Tovar, S., Raghay, K., Rodríguez-Cuenca, S., Deoliveira, R.M., Castañeda, T., Datta, R., Dong, J.Z., Culler, M., Sleeman, M.W., Alvarez, C.V., Gallego, R., Lelliott, C.J., Carling, D., Tschöp, M.H., Diéguez, C., Vidal-Puig, A., 2008. Hypothalamic fatty acid metabolism mediates the orexigenic action of ghrelin. Cell Metab. 7 (5), 389–399. https://doi.org/10.1016/j.cmet.2008.03.006.
Luan, X., Sun, X., Guo, F., Zhang, D., Wang, C., Ma, L., Xu, L., 2017. Lateral hypothalamic orexin-A-ergic projections to the arcuate nucleus modulate gastric function in vivo. J. Neurochem. 143 (6), 697–707. https://doi.org/10.1111/jnc.14233.
Lv, Z., Gao, J., Wang, L., Chen, Z., Yuan, H., Ma, X., Lu, J., Lv, J., Wu, X., Zhang, L., Wei, L., Xue, R., Fu, R., Ma, L., 2016. Uremia-caused changes of ghrelin system in hippocampus may be associated with impaired cognitive function of hippocampus. Int. Urol. Nephrol. 48 (5), 807–815. https://doi.org/10.1007/s11255-016-1228-9.
Lv, Y., Liang, T., Wang, G., Li, Z., 2018. Ghrelin, a gastrointestinal hormone, regulates energy balance and lipid metabolism. Biosci. Rep. 38 (5), BSR20181061. https://doi.org/10.1042/BSR20181061.
Martins, L., Fernández-Mallo, D., Novelle, M.G., Vázquez, M.J., Tena-Sempere, M., Nogueiras, R., López, M., Diéguez, C., 2013. Hypothalamic mTOR signaling mediates the orexigenic action of ghrelin. PLoS One 7 (10), e46923. https://doi.org/10.1371/journal.pone.0046923.
Mondal, M.S., Date, Y., Yamaguchi, H., Toshinai, K., Tsuruta, T., Kangawa, K., Nakazato, M., 2005. Identification of ghrelin and its receptor in neurons of the rat arcuate nucleus. Regul. Pept. 126 (1–2), 55–59. https://doi.org/10.1016/j.regpep.2004.08.038.
Morgan, K., Obici, S., Rossetti, L., 2004. Hypothalamic responses to long-chain fatty acids are nutritionally regulated. J. Biol. Chem. 279 (30), 31139–31148. https://doi.org/10.1074/jbc.M400458200.
Müller, T.D., Nogueiras, R., Andermann, M.L., Andrews, Z.B., Anker, S.D., Argente, J., Batterham, R.L., Benoit, S.C., Bowers, C.Y., Broglio, F., Casanueva, F.F., D'Alessio, D., Depoortere, I., Geliebter, A., Ghigo, E., Cole, P.A., Cowley, M., Cummings, D.E., Dagher, A., Diano, S., Dickson, S.L., Diéguez, C., Granata, R., Grill, H.J., Grove, K., Habegger, K.M., Heppner, K., Heiman, M.L., Holsen, L., Holst, B., Inui, A., Jansson, J.O., Kirchner, H., Korbonits, M., Laferrère, B., LeRoux, C.W., Lopez, M., Morin, S., Nakazato, M., Nass, R., Perez-Tilve, D., Pfluger, P.T., Schwartz, T.W., Seeley, R.J., Sleeman, M., Sun, Y., Sussel, L., Tong, J., Thorner, M.O., van der Lely, A.J., van der Ploeg, L.H., Zigman, J.M., Kojima, M., Kangawa, K., Smith, R.G., Horvath, T., Tschöp, M.H., 2015. Ghrelin. Mol. Metab. 4 (6), 437–460. https://doi.org/10.1016/j.molmet.2015.03.005.
Murtuza, M.I., Isokawa, M., 2017. Endogenous ghrelin-O-acyltransferase (GOAT) acylates local ghrelin in the hippocampus. J. Neurochem. 144 (1), 58–67. https://doi.org/10.1111/jnc.14244.
Paeger, L., Karakasilioti, I., Altmüller, J., Frommolt, P., Brüning, J., Kloppenburg, P., 2017. Antagonistic modulation of NPY/AgRP and POMC neurons in the arcuate nucleus by noradrenalin. eLife 6, e25770. https://doi.org/10.7554/eLife.25770.
Paxinos, G., Watson, C., 2008. The Rat Brain in Stereotaxic Coordinates.
Pocai, A., Obici, S., Schwartz, G.J., Rossetti, L., 2005. A brain–liver circuit regulates glucose homeostasis. Cell Metab. 1 (1), 53–61. https://doi.org/10.1016/j.cmet.2004.11.001.
Poher, A.L., Tschöp, M.H., Müller, T.D., 2018. Ghrelin regulation of glucose metabolism. Peptides 100, 236–242. https://doi.org/10.1016/j.peptides.2017.12.015.
Poykko, S.M., Kellokoski, E., Horkko, S., Kauma, H., Kesaniemi, Y.A., Ukkola, O., 2003. Low plasma ghrelin is associated with insulin resistance, hypertension, and the prevalence of type 2 diabetes. Diabetes 52 (10), 2546–2553. https://doi.org/10.2337/diabetes.52.10.2546.
Pustovit, R.V., Callaghan, B., Ringuet, M.T., Kerr, N.F., Hunne, B., Smyth, I.M., Pietra, C., Furness, J.B., 2017. Evidence that central pathways that mediate defecation utilize ghrelin receptors but do not require endogenous ghrelin. Physiol. Rep. 5 (15). https://doi.org/10.14814/phy2.13385. pii: e13385.
Routh, V.H., 2002. Glucose-sensing neurons: are they physiologically relevant? Physiol. Behav. 76 (3), 403–413. https://doi.org/10.1016/S0031-9384(02)00761-8.
Russo, C., Russo, A., Gulino, R., Pellitteri, R., Stanzani, S., 2017a. Effects of different musical frequencies on NPY and ghrelin secretion in the rat hypothalamus. Brain Res. Bull. 132, 204–212. https://doi.org/10.1016/j.brainresbull.2017.06.002.
Russo, C., Russo, A., Pellitteri, R., Stanzani, S., 2017b. Hippocampal ghrelin-positive neurons directly project to arcuate hypothalamic and medial amygdaloid nuclei. Could they modulate food-intake? Neurosci. Lett. 653, 126–131. https://doi.org/10.1016/j.neulet.2017.05.049.
Sangiao-Alvarellos, S., Varela, L., Vázquez, M.J., Da Boit, K., Saha, A.K., Cordido, F., Diéguez, C., López, M., 2010. Influence of ghrelin and growth hormone deficiency on AMP-activated protein kinase and hypothalamic lipid metabolism. J. Neuroendocrinol. 22 (6), 543–556. https://doi.org/10.1111/j.1365-2826.2010.01994.x.
Sato, T., Fukue, Y., Teranishi, H., Yoshida, Y., Kojima, M., 2005. Molecular forms of hypothalamic ghrelin and its regulation by fasting and 2-deoxy-d-glucose administration. Endocrinology 146 (6), 2510–2516. https://doi.org/10.1210/en.2005-0174.
Scott, M.M., Perello, M., Chuang, J.C., Sakata, I., Gautron, L., Lee, C.E., Lauzon, D., Elmquist, J.K., Zigman, J.M., 2012. Hindbrain ghrelin receptor signaling is sufficient to maintain fasting glucose. PLoS One 7 (8), e44089. https://doi.org/10.1371/journal.pone.0044089.
Spiegel, K., Tasali, E., Leproult, R., Scherberg, N., Van, C.E., 2011. Twenty-four-hour profiles of acylated and total ghrelin: relationship with glucose levels and impact of time of day and sleep. J. Clin. Endocrinol. Metab. 96 (2), 486–493. https://doi.org/10.1210/jc.2010-1978.
Stark, R., Reichenbach, A., Lockie, S.H., Pracht, C., Wu, Q., Tups, A., Andrews, Z.B., 2015. Acyl ghrelin acts in the brain to control liver function and peripheral glucose homeostasis in male mice. Endocrinology 156 (3), 858–868. https://doi.org/10.1210/en.2014-1733.
Steculorum, S.M., Collden, G., Coupe, B., Croizier, S., Lockie, S., Andrews, Z.B., Jarosch, F., Klussmann, S., Bouret, S.G., 2015. Neonatal ghrelin programs development of hypothalamic feeding circuits. J. Clin. Investig. 125 (2), 846–858. https://doi.org/10.1172/JCI73688.
Sun, Y., Asnicar, M., Smith, R.G., 2007. Central and peripheral roles of ghrelin on glucose homeostasis. Neuroendocrinology 86 (3), 215–228. https://doi.org/10.1159/000109094.
Van, D.L., Tschöp, M., Heiman, M.L., Ghigo, E., 2004. Biological, physiological, pathophysiological, and pharmacological aspects of ghrelin. Endocr. Rev. 25 (3), 426–457. https://doi.org/10.1210/er.2002-0029.
Varela, L., Vázquez, M.J., Cordido, F., Nogueiras, R., Vidal-Puig, A., Diéguez, C., López, M., 2011. Ghrelin and lipid metabolism: key partners in energy balance. J. Mol. Endocrinol. 46 (2), R43–R63. https://doi.org/10.1677/JME-10-0068.
Velásquez, D.A., Martinez, G., Romero, A., Vázquez, M.J., Boit, K.D., Dopeso-Reyes, I.G., López, M., Vidal, A., Nogueiras, R., Diéguez, C., 2011. The central sirtuin1/p53 pathway is essential for the orexigenic action of ghrelin. Diabetes 60 (4), 1177–1185. https://doi.org/10.2337/db10-0802.
Wang, W.G., Chen, X., Jiang, H., Jiang, Z.Y., 2008. Effects of ghrelin on glucose-sensing and gastric distension sensitive neurons in rat dorsal vagal complex. Regul. Pept. 146 (1–3), 169–175. https://doi.org/10.1016/j.regpep.2007.09.007.
Enriori, P.J., Wilson, J.L., 2015. A talk between fat tissue, gut, pancreas and brain to control body weight. Mol. Cell. Endocrinol. 418 (Pt 2), 108–119. https://doi.org/10.1016/j.mce.2015.08.022.
Xu, L., Gong, Y., Wang, H., Sun, X., Guo, F., Gao, S., Gu, F., 2014. The stimulating effect of ghrelin on gastric motility and firing activity of gastric-distension-sensitive hippocampal neurons and its underlying regulation by the hypothalamus. Exp. Physiol. 99 (1), 123–135. https://doi.org/10.1113/expphysiol.2013.074716.
Zagmutt, S., Mera, P., Soler-Vázquez, M.C., Herrero, L., Serra, D., 2018. Targeting AgRP neurons to maintain energy balance: lessons from animal models. Biochem. Pharmacol. 155, 224–232. https://doi.org/10.1016/j.bcp.2018.07.008.
Zhang, W., Lin, T.R., Hu, Y., Fan, Y., Zhao, L., Stuenkel, E.L., Mulholland, M.W., 2004. Ghrelin stimulates neurogenesis in the dorsal motor nucleus of the vagus. J. Physiol. 559 (Pt 3), 729–737. https://doi.org/10.1113/jphysiol.2004.064121.
Zhao, T.J., Liang, G., Li, R.L., Xie, X., Sleeman, M.W., Murphy, A.J., Valenzuela, D.M., Yancopoulos, G.D., Goldstein, J.L., Brown, M.S., 2010. Ghrelin o-acyltransferase (goat) is essential for growth hormone-mediated survival of calorie-restricted mice. Proc. Natl. Acad. Sci. U. S. A. 107 (16), 7467–7472. https://doi.org/10.1073/pnas.1002271107.
Zigman, J.M., Jones, J.E., Lee, C.E., Saper, C.B., Elmquist, J.K., 2006. Expression of ghrelin receptor mRNA in the rat and the mouse brain. J. Comp. Neurol. 494 (3), 528–548. https://doi.org/10.1002/cne.20823.